



CO₂ capture over steam and KOH activated biochar: Effect of relative humidity

Chen Zhang^a, Shuzhuang Sun^a, Shaojun Xu^{b,c,**}, Chunfei Wu^{a,*}

^a School of Chemistry and Chemical Engineering, Queens University Belfast, Belfast, BT7 1NN, UK

^b School of Chemistry, Cardiff University, Cardiff, CF10 3AT, UK

^c UK Catalysis Hub, Research Complex at Harwell, Didcot, OX11 0FA, UK

ARTICLE INFO

Keywords:

Biomass
Biochar
Wood pellet
Carbon capture
Relative humidity

ABSTRACT

Carbon dioxide (CO₂) capture is critical for emission reduction. Biochar is a promising adsorbent for CO₂ capture. In this work, the effect of relative humidity and biochar activation with steam or KOH treatment on CO₂ capture was investigated. The results demonstrate that the biochar sample activated by KOH has a high CO₂ capture capacity (50.73 mg g⁻¹). In addition, the biochar after 1.0 h of steam treatment showed a carbon capture capacity of 38.84 mg g⁻¹. The results also show that the capture ability of biochar decreased as CO₂ concentration decreased from 100% to 15%. The relative humidity had a negative impact on CO₂ capture over biochar. The CO₂ capture capability of biochar materials treated by steam decreased by a range of 31.38%–62.89% as the relative humidity rose from 8.8% to 87.9%. Furthermore, the lifetime of biochar samples at various relative humidity shows that increased relative humidity had a negative impact on CO₂ adsorption due to water molecules occupying active sites.

1. Introduction

The increasing concentration of carbon dioxide (CO₂) results in the challenges of climate change, especially the extreme weather phenomenon [1]. As a result, significant efforts have been made to reduce CO₂ emissions, and carbon capture, such as membrane separation, solvent absorption, and sorbent adsorption, is one of the most promising technologies [2,3]. Amine solution as a liquid phase sorbent is the current industry practice for CO₂ capture. Despite being considered a state-of-the-art process, it has a large energy penalty, and the sorbent is corrosive to instruments [4,5]. Compared to amine-based sorbents, solid sorbents have the advantages of lower capital costs, higher efficiency, and less waste generation [6,7].

Among the reported solid sorbents (such as MOFs [8] and silica [9]) for carbon capture, biochar produced from biomass pyrolysis under an inert atmosphere with a low capital cost has attracted extensive attention [10]. Biomass materials used to produce biochar are calcined (also known as pyrolysis) at moderate temperatures (generally lower than 700° Celsius) in an anaerobic or infinitesimal-oxygen atmosphere to produce porous biochar materials with high carbon content and multiple elements [11]. Wood-derived biochar has been regarded as high carbon

content material [12], illustrating a high potential for biochar activation and modification. Significantly, Lehmann [13] estimated that the utilization of biochar as sorbents has the potential to absorb up to 1 gigatonne (Gt) of greenhouse gases per year, which was more than 10% of total global emissions. Coincidentally, the reason why biochar has such a promising future application in carbon capture is that it has the majority advantages: 1) numerous biomass wastes can be used as the feedstock of biochar production, such as agricultural waste, animal husbandry waste, and municipal sludge [12]; 2) further application of spent biochar can be utilized in other fields like wastewater treatment [14] and glass production [15] to achieve the maximum utilization efficiency; 3) Biochar shows more desirable adsorption properties when applied to bulk gas adsorption applications due to its cost and environmental sustainability compared to organic chemicals such as MOFs [16]; 4) Biochar can be highly malleable according to the different activation processes. Here, surface area, porosity, and surface functional groups all need to be addressed to improve CO₂ capture.

Chemical and physical activation is typically applied for biochar activation to enhance CO₂ capture capacity and improve surface properties. Chemical activation uses acids (e.g., H₃PO₄ and H₂SO₄) [17,18], strong alkalines (e.g., KOH and NaOH) [19,20], or salts [21] as activation agents, resulting in high surface area and porosity. Chemical

* Corresponding author.

** Corresponding author. School of Chemistry, Cardiff University, Cardiff, CF10 3AT, UK.

E-mail addresses: xus25@cardiff.ac.uk (S. Xu), c.wu@qub.ac.uk (C. Wu).

<https://doi.org/10.1016/j.biombioe.2022.106608>

Received 23 May 2022; Received in revised form 12 September 2022; Accepted 18 September 2022

Available online 25 September 2022

0961-9534/© 2022 The Authors. Published by Elsevier Ltd. This is an open access article under the CC BY license (<http://creativecommons.org/licenses/by/4.0/>).

Abbreviations

MOF	metal organic framework
TGA	thermal gravity analysis
TPO	temperature programmed oxidation
BET	Brunauer-Emmett-Teller
SEM	scanning electron microscopy
ATR-FTIR	attenuated total reflection - Fourier transform infrared spectroscopy

activation is more efficient than physical activation in creating biochar porosity, but it has a more complex technique and higher expense, as well as the possibility of secondary environmental pollutants [10]. Biochar samples generally need to be brought into complete contact with the alkaline agents at room temperature by physical mixing or impregnation before calcination at high temperatures (300 °C–700 °C), and the unstable carbonous char corrodes during the reaction and generates a porous structure. In comparison, physical activation uses inorganic compounds as the activation agents, such as H₂O [22] and CO₂ [23]. Typically, steam activation is a process whereby the introduced water molecules enter the internal structure of the biochar and react with the unstable char to produce gases such as carbon monoxide, which is a simple process that is extremely friendly to the environment. Furthermore, the reported activation conditions for steam activation are basically at a higher temperature and longer duration time [24]. Moreover, the surface area of the same biochar increases as the physical activation temperature rises for the same activation time, which is because the activation process is a heat absorbing (endothermic, $\Delta H < 0$) reaction [25] and the higher the temperature, the more intense the reaction, which is more favourable to biochar pore formation. In addition, the activation residence time is also a significant influence. Theoretically, the longer the activation time, the more the carbon reacts to the water vapor, but Demiral [26] has shown that redundant activation time can lead to a breakdown of the porous structure and thus a decrease in the specific surface area. Therefore, the activation process of biochar is characterized by several factors that need to be considered and the compatible activation conditions found.

Nevertheless, various activation methods would produce more suitable properties for carbon capture. The works commonly reported that the adjustment of microporosity is more necessary for high CO₂ adsorption performance among surface morphology properties [27]. For example, KOH-activated bamboo charcoal demonstrates a 15% CO₂ adsorption capacity of 1.50 mmol g⁻¹ at 25 °C [28]. Also, wood-pellet/food waste biochar activated with KOH and CO₂ show a CO₂ adsorption capacity of ~1.22 mmol g⁻¹ and ~1.18 mmol g⁻¹ at 25 °C, respectively [29]. However, the previous works did not investigate the correlation between textural properties and CO₂ capture performance. Therefore, it is necessary to introduce more performance about steam- and KOH-activated wood-pellet biochar applied in carbon capture. Additionally, concerning the application of biochar as the sorbent for carbon capture, some factors such as raw materials, temperature, pressure, and humidity can affect the performance of CO₂ capture [30,31]. Although studies have shown that temperature and pressure greatly influenced CO₂ capture [29,32], few studies have explored the influence of relative humidity (RH) in CO₂ sources on biochar adsorption performance. It is noted that RH is an important factor in the practical application of carbon capture using biochar. The moisture content is known and varies from 150 to 108 g per kilogram of dry gas in the industrial exhausted flue gas. A few studies investigated the influence of RH on carbon capture using solid sorbents, such as activated carbon fibers (ACF) [33] and metal-organic frameworks (MOFs). Their results showed that the relative humidity weakened CO₂ capture due to the competition from CO₂ adsorption by H₂O [34]. A humid

environment increased the swelling of polymer membranes (CO₂ sorbent) and caused the reduced efficiency of CO₂ capture [35]. However, to our best knowledge, the influence of RH on CO₂ capture using biochar-based sorbents has not been well understood under different conditions.

Herein, this work investigated the influence of relative humidity on the CO₂ capture capacity over biochar using thermogravimetric analysis (TGA) and fix-bed reactors. More importantly, the effect of biochar with different properties after activation using KOH and steam was studied to understand the relationship between the properties of biochar and the CO₂ adsorption to achieve the desired properties of biochar to enhance the CO₂ capture capacity in the presence of water. In addition, the stability of biochar under different humidity conditions was investigated to investigate the working life of BC-Steam-1.0h for CO₂ capture.

2. Experimental

2.1. Activation of the biochar

The biochar (BC) used in this work was produced from EN1 Grade A wood pellets by Energetgreen Ltd. The precursor (BC-Raw) was sieved with a size below 500 μm and dried in an oven overnight at 105 °C. The dried sample was named as BC-Raw. For the biochar activation, around 5 g BC-Raw was placed into a fixed bed reactor and then heated to 850 °C at a nitrogen gas flow rate of 100 ml min⁻¹.

For steam activation, a syringe pump was used to introduce water at a flow rate of 10 ml h⁻¹ to introduce water vapor carried by nitrogen gas at a gas flow rate of 100 ml min⁻¹. The activation temperature was set at 850 °C, while the activation time was varied with 0.5, 1, and 1.5 h, where the derived samples were denoted as BC-Steam-0.5h, BC-Steam-1.0h, and BC-Steam-1.5h, respectively. For the chemical activation, the biochar sample was physically mixed with solid potassium hydroxide in a mass ratio of 2:1 and 1:1 by grinding with a mortar and pestle. Afterward, the sample was calcined at 850 °C for 1 h in a tube furnace under an N₂ atmosphere of 100 ml min⁻¹. Finally, the sample was washed with deionized water until PH neutral and dried at 110 °C for 8 h. The obtained samples with biochar and KOH mass ratios of 2:1 and 1:1 were denoted as BC-KOH-2:1 and BC-KOH-1:1, respectively. For comparison, KOH solution was impregnated on dried wood-pellet biochar at a mass ratio of 1:1 for 4 h to investigate the effect of different KOH activation methods. That dried biochar sample was then calcinated at 850 °C for 1 h under N₂ atmosphere (100 ml min⁻¹), noted as BC-KOH-Imp.

2.2. Biochar characterization

The elemental analysis (composition of C, H, and N) of the biochar samples was carried out using CHNS Element Analyser (PerkinElmer PE2400). Temperature programmed oxidation (TPO) analysis was tested by TA Instruments TGA 2950 thermogravimetric analyzer (TGA) under an air atmosphere to measure moisture, ash, and volatile matter contents. 20 mg sample was heated to 850 °C at 10 °C min⁻¹ under N₂ flowing (100 ml min⁻¹) to obtain the content of moisture and volatiles. The presence of functional and aromatic groups on the surface of biochar samples was determined by ATR-FTIR (PerkinElmer Spectrum II Spectrometer), and the spectra in the range of 3000–1400 cm⁻¹ band were analyzed. The surface morphology and pore structure of the material was determined by scanning electron microscope (SEM) using JEOL JSM-6610LV, and the distribution of elements on the surface of samples was monitored by Energy Dispersive X-Ray Analyser (SEM-EDX). Surface area, pore volume, and the specific surface area (BET) and pore structure were measured with a Quantachrome instrument, using the adsorption of N₂ at the liquid nitrogen temperature.

2.3. CO₂ capacity test

Fig. 1 shows the schematic diagram of the process of CO₂ capture. Carbon capture was carried out at room temperature (25 °C) using a horizontal tube furnace. Around 1 g activated biochar sample was placed in a quartz tube (20 mm out diameter and 600 mm length) with a gas flow rate of 100 ml min⁻¹ under pure CO₂ or 15% CO₂ (contained 85% N₂) selected as the simulated flue gases. CO₂ was bubbled through the humidity control system to introduce moisture into the sorbent-contained quartz tube. The value of RH was adjusted by using a RH regulator using an ice and water bath to control the temperature. During the desorption of CO₂, the temperature was increased to 70 °C to release the captured CO₂ and regenerate the biochar. The concentration of CO₂ during the process was analyzed with a Kane 457 gas analyzer. The capacity of CO₂ capture (C_m) was calculated according to the integral area (S) after subtracting the dead volume, as shown in Eq. (1):

$$C_m = \frac{S^* \gamma^* M_{CO_2}}{V_m^* M_{BC}} \quad (1)$$

where γ is the gas flow rate; M_{CO_2} is molecular weight 44.01 g mol⁻¹; V_m is gas molar volume 22.4 L mol⁻¹; M_{BC} is mass of added biochar sorbent.

3. Results and discussion

3.1. Characterization of wood pellet derived biochar

The results of the proximate analysis and element analysis of the biochar samples are shown in Fig. 2(a) and Table 1. The weight loss of the samples is addressed in Fig. 2 (a). As shown in Table 1, for the biochar samples produced from different activation conditions, the contents of fixed carbon are similar, which are between 82.34% and 89.99%. In the meantime, it can be seen from the element analysis in Table 1 that the amounts of carbon in all the biochar samples account are from 81.57% to 88.01%, whilst the other elements are relatively low. Compared with the other reported biomass feedstock (such as digestate and sludge with 33.55% and 38.94% of C) [29], the biochar used in this work has a higher carbon content, which may be related to the pre-treatment of wood pellet.

The reduction of volatile matter contents after pyrolysis is ascribed to the oxidation reaction between volatiles of biochar and steam or KOH [36]. In addition, it is noted that the BC-KOH-Imp sample prepared by impregnating KOH solution on raw biochar shows the highest ash content of 37.98%. The main components of ash are metal oxide, carbon, and silica [37]. Compared to the physical dry mixed KOH treatment, organic matter in biochar could be removed entirely by KOH solution during impregnation, and K-contained chemicals could react with

carbon sufficiently, which results in the high ash content of BC-KOH-Imp. According to the literature, the increasing composition of ash might be due to the introduction of KOH [20], and potassium oxide in BC-KOH-Imp was more difficult to be removed than BC-KOH-1:1.

To further analyze surface morphology, the ATR-FTIR analysis was carried out. The results are shown in Fig. 2(b). It can be seen the presence of abundant oxygen-containing and carbon-based functional groups on the surface of the biochar samples. The C=O groups on each sample at the wavelength range of 2000–1650 cm⁻¹ are assigned to the aromatic C–H group bending. Moreover, the peaks in the range of 2400–2000 cm⁻¹ corresponded to the central double bond groups, such as O=C=O, C=N, C=C=C. In addition, compared to other biochar or activated carbons, wood-pellet biochar showed less intensity in the range of 3500–2500 cm⁻¹, because the surface functional groups (e.g., –OH at ~3500 cm⁻¹) were relatively stable under the high-temperature (850 °C) activation [39].

The morphology of the biochar samples is further analyzed using scanning electron microscopy (SEM) in Fig. 3. The BC-Raw sample demonstrated a rough and microporous surface (Fig. 3(a)). After activating the raw biochar sample by steam, the surface of the sample shows uniform tubular structures across the biochar surface (Fig. 3(b–d)). Fig. 4(e–f) shows that chemical activation using KOH could also lead to the generation of pores inside the biochar samples, providing a tubular structure. However, it seems that the surface structure of BC-KOH-1:1 (Fig. 3 (f)) was destroyed by the over-reaction between excess KOH and biochar.

The surface and porosity properties of the biochar samples were tested using the low-temperature N₂ adsorption, as shown in Table 2 and Fig. 4. It shows that the raw biochar material (BC-Raw) exhibited a specific surface area of 130.5 m² g⁻¹ and a pore volume of 0.17 cm³ g⁻¹. After the activation by different methods, a significantly increased surface area of 854.7 m² g⁻¹ (BC-Steam-1.0h) and 713.5 m² g⁻¹ (BC-KOH-1:1) was observed. It is noted that the specific surface area of the biochar derived from wood pellet in this study is higher compared to other reported biochar using the same activation method (such as whitewood biochar with 664 m² g⁻¹) [20]. Additionally, the surface area of the steam-activated biochar is decreased when the duration time was extended from 1.0 h to 1.5h, which illustrates the possibility of a reduction in surface area due to the over-activation [26]. The BC-Raw sample exhibited an average pore diameter of 52.37 Å, and steam-activated samples show higher pore diameters of 36.62–42.05 Å than the KOH-activated biochar. However, biochar samples activated by KOH show the smallest average pore diameters compared to other BC samples. In contrast, three KOH activated biochar exhibit a higher ratio of S_{micro} versus S_{meso} (Table 2) and more mesopores (Fig. 4(b)), which is consistent with the report that micropores, mesopores, and micro/meso combined pores could be generated during KOH activation [19,20].

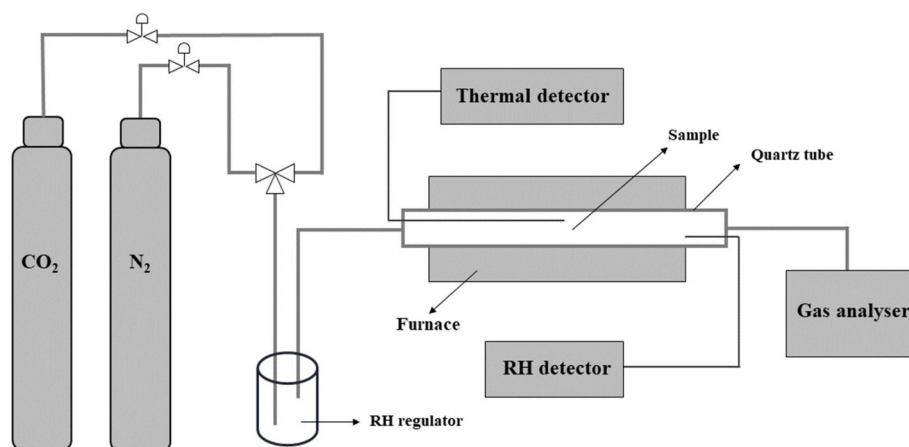


Fig. 1. Schematic illustration of the setup used for CO₂ adsorption and desorption.

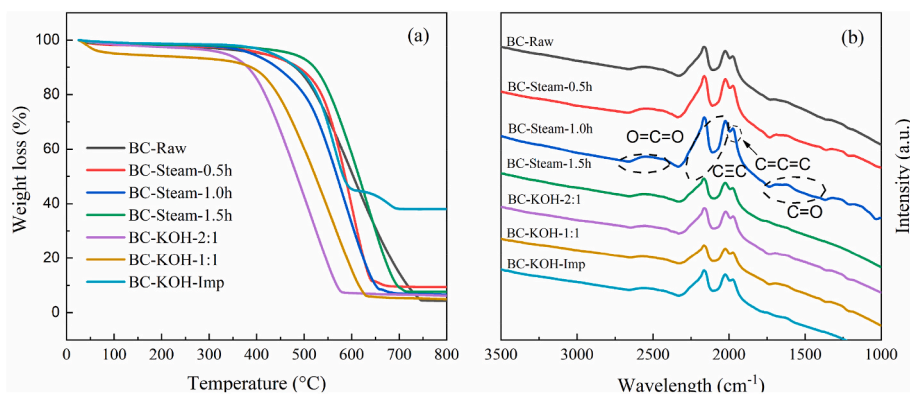


Fig. 2. (a) TGA-TPO and (b) ATR-FTIR spectrums of biochar samples.

Table 1

Proximate analysis results and element analysis of CHNS contents.

Sample	Proximate Analysis (wt. %)				Elements Analysis (wt. %)				
	Moisture	Volatile matter	Fixed carbon	Ash	C	H	N	S	O ^a
BC-Raw	1.53	7.48	86.17	4.71	88.01	1.14	0.33	<0.30	10.22
BC-Steam-0.5h	2.26	4.54	83.80	9.40	86.56	0.47	<0.30	<0.30	12.37
BC-Steam-1.0h	1.87	2.83	88.81	6.62	81.64	0.69	0.34	<0.30	16.31
BC-Steam-1.5h	1.73	3.33	87.28	7.66	87.65	0.76	<0.30	<0.30	10.99
BC-KOH-2:1	2.62	8.81	82.34	6.29	84.17	0.70	0.51	<0.30	14.32
BC-KOH-1:1	1.24	6.38	89.99	2.38	81.57	0.68	0.54	<0.30	16.91
BC-KOH-Imp	1.27	5.48	55.27	37.98	84.86	0.48	<0.30	<0.30	14.06

^a Oxygen content was obtained by weight differences [32,38].

3.2. CO₂ adsorption performance using different biochar samples

The CO₂ adsorption test using the prepared activated biochar samples was carried out over both 15% and 100% CO₂ concentrations CO₂. As shown in Fig. 5 (a), the raw biochar (BC-Raw) sample shows the lowest capacity of CO₂ capture, which is 10.45 mg g⁻¹ for 15% CO₂ capture and 22.16 mg g⁻¹ for 100% CO₂ capture. The capacity of CO₂ capture over the BC-Raw sample is increased over the sample after activation treatment. For example, 15% CO₂ capture capacity is increased to 11.44–25.50 mg g⁻¹ for steam-activated biochar and 20.60–50.75 mg g⁻¹ for KOH-activated biochar. As expected, the biochar adsorbents show around 50% higher carbon capture capacity in a 100% CO₂ atmosphere than in a 15% CO₂. The higher partial pressure of CO₂ benefits the adsorption of CO₂ in biochar [29].

For comparing the activation conditions, the CO₂ capture capacities of the steam-activated biochar samples are decreased from 38.30 mg g⁻¹ to 26.60 mg g⁻¹ in a pure CO₂ atmosphere with the increase of steam activation time from 0.5 h to 1.5 h. It is suggested that CO₂ adsorption capacity was closely related to biochar morphology which was affected by the activation time. Especially, the micropores show a crucial role in carbon capture [40], which is in line with the results obtained in Table 2 and Fig. 5(c) and (e). According to the results from Plaza et al. [41], the CO₂ adsorption capacities of the evaluated samples decreased as temperature and activation time increased. Fundamentally, activation time shows a clear effect on biochar surface texture, and CO₂ capture capacities can be affected due to the morphology variation. However, based on the obtained results, the BET surface area, mesopore surface area, and total pore volume are not directly related to carbon capture capacity. A previous study suggested the effect of calcination time on activated carbon pore size distribution [42], and the micropores volume below 0.6 nm was an important influence factor on low-temperature carbon capture [43]. In the meanwhile, due to the different average pore diameters caused by different activation time and methods (shown in Table 2), it has also been reported that CO₂ adsorption behavior is related to average pore diameter [41,43]. Therefore, the factors that

determine the CO₂ adsorption capacity of biochars are complex, but micropores are crucial in the role of CO₂ capture.

In particular, the biochar samples activated by KOH show a higher capability for carbon capture compared to the steam-activated biochar samples. As shown in Fig. 5 (a), when the biochar sample was changed from BC-Raw to BC-KOH-1:1, the capacity of CO₂ capture increase from 10.45 mg g⁻¹ to 25.50 mg g⁻¹ at 15% CO₂ and 22.16 mg g⁻¹ to 50.75 mg g⁻¹ at pure CO₂. Although steam activation and KOH activation were accomplished by removing carbonaceous species from biochar to change biochar morphology [19], KOH could also adjust the pH of biochar adsorbents [44]; the introduction of alkaline species could enhance the absorption of CO₂. Furthermore, BC-KOH-1:1 shows a slightly higher CO₂ capture capacity than BC-KOH-2:1. The work from Hong [45] demonstrated that biochar activated by a higher dosage of KOH had higher CO₂ capture ability due to the high concentration of KOH. It is indicated that the morphology and porosity of biochar might not be a dominant factor for carbon capture for the KOH-activated biochar samples. Therefore, the increase in KOH/C mass ratio enhances the specific surface area, total pore volume, and micropore volume, supporting the increase of the capacity of CO₂ capture with the increase of KOH addition [45,46].

3.3. Influence of relative humidity on CO₂ capture

The influence of relative humidity (8.8%, 30.7%, and 87.9%) on carbon capture was further investigated using a 15% CO₂ concentration. As shown in Fig. 6, at 8.8% relative humidity, the chemical activation produced biochar samples show a higher adsorption capacity than the steam-activated biochar samples. For example, BC-KOH-Imp shows the highest CO₂ capture capacity (3.69 mg g⁻¹). Moreover, with increasing relative humidity, the capacity of CO₂ capture is significantly reduced, particularly for the biochar samples activated by KOH. For example, the adsorption ability of BC-KOH-1:1 and BC-KOH-Imp decreased by 62.89% and 61.17%, respectively, when the RH was increased from 8.8% RH to 87.9% RH. In general, the presence of a high water vapor

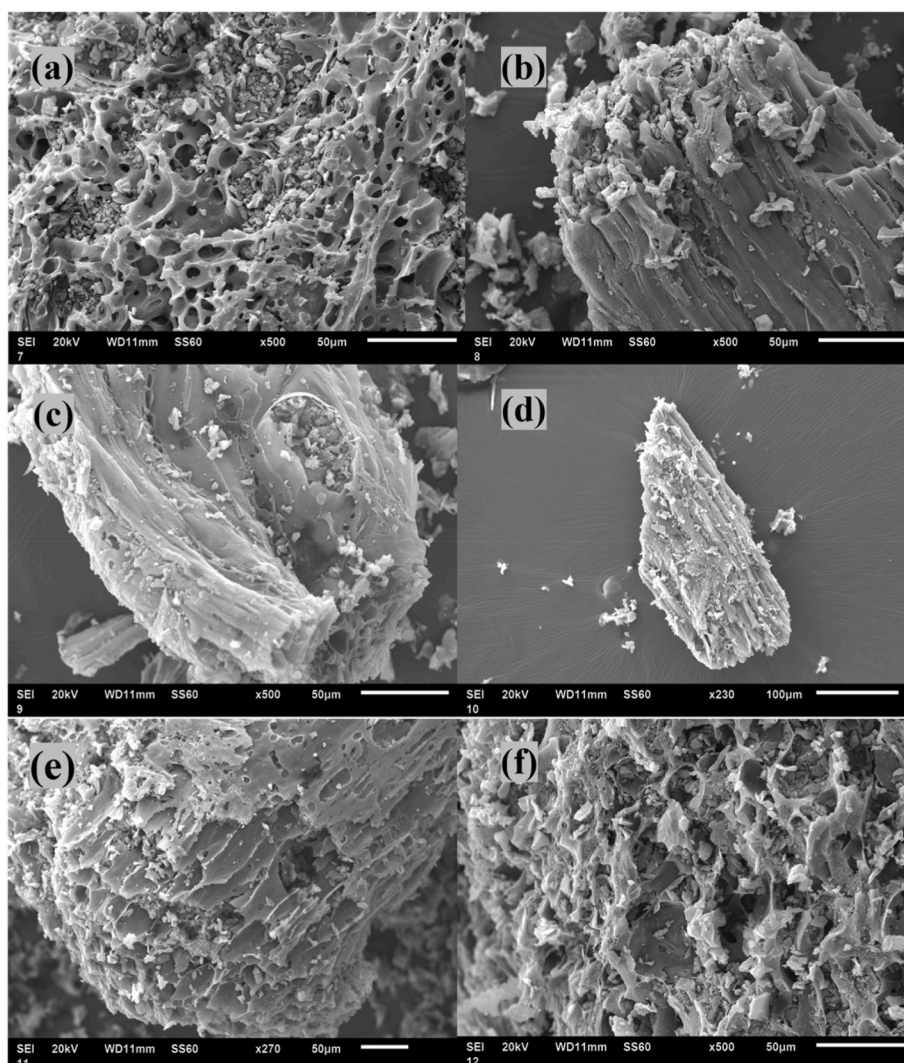


Fig. 3. SEM micrograph of (a) BC-Raw, (b) BC-Steam-0.5h, (c) BC-Steam-1.0h, (d) BC-Steam-1.5h, (e) BC-KOH-2:1, and (f) BC-KOH-1:1.

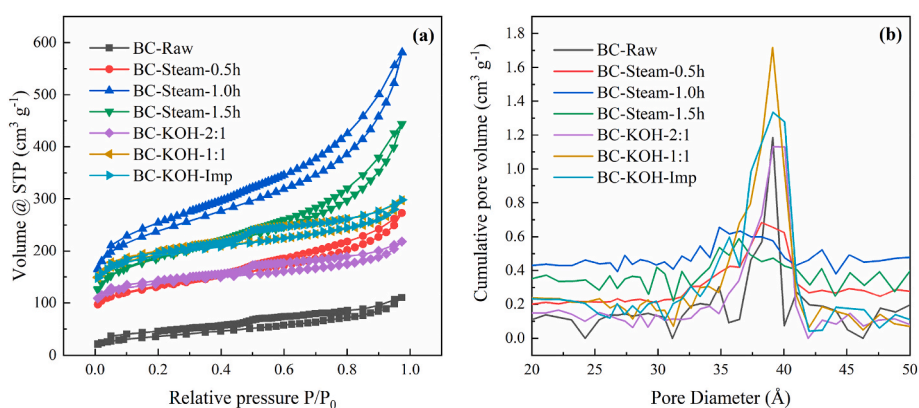


Fig. 4. (a) Nitrogen adsorption-desorption BET isotherm of wood pellet biochar samples; (b) pore distribution of wood pellet biochar samples.

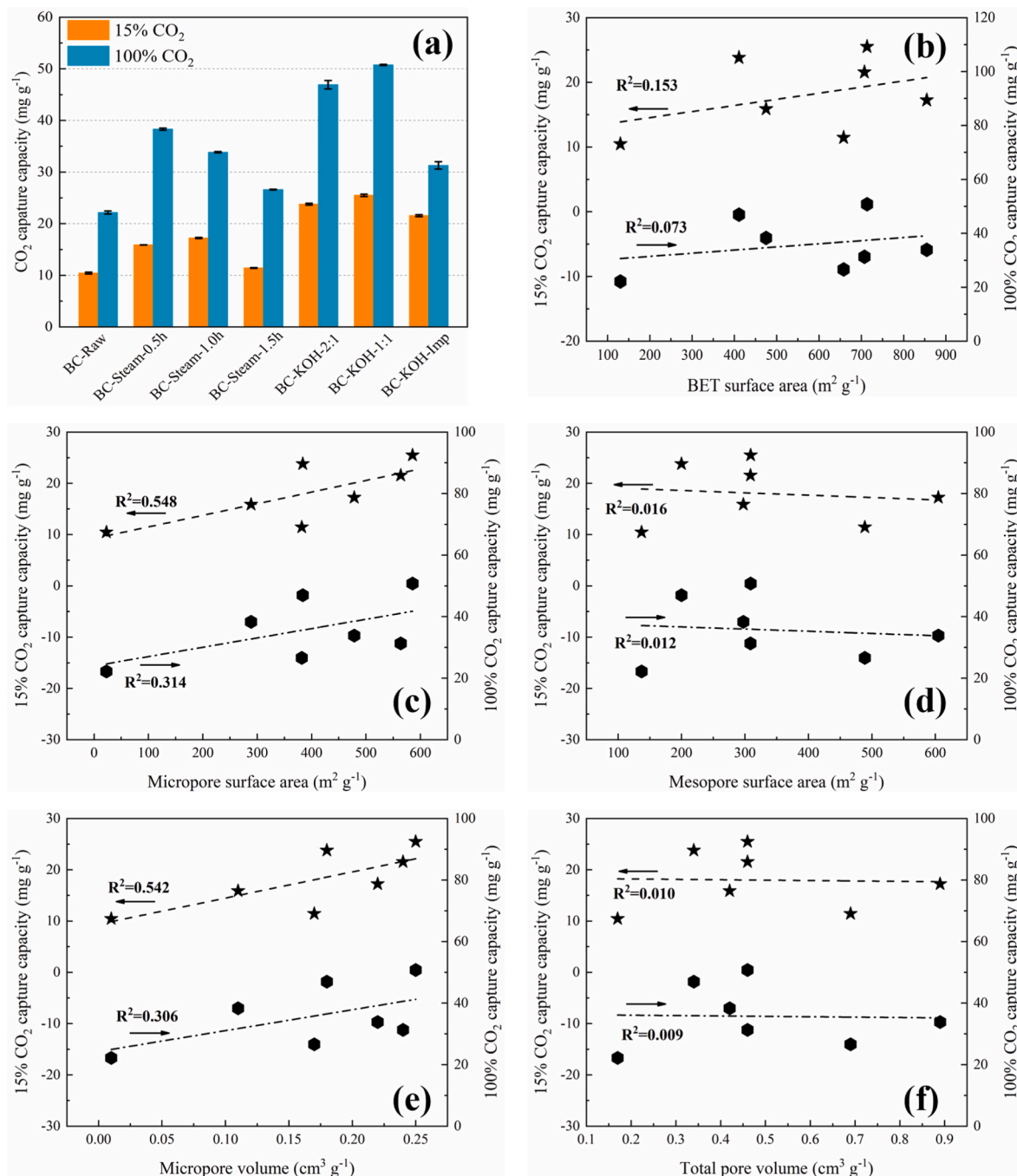
concentration in the introduced CO_2 gas interferes with the CO_2 adsorption by biochar samples [47]. Previous studies suggested that CO_2 capture capacity using porous adsorbents was affected under humid conditions; the adsorption capacity of the sorbents under moisture could be reduced by 73% compared to dry conditions [34]. It is suggested that water molecules have higher polarity and binding energy with adsorbents, resulting in the occupation of the active sites of sorbent [33,48].

Interestingly, although the steam-activated biochar samples have a lower CO_2 capture capacity than the chemical activation samples, the increase of RH shows a minor influence on the steam-activated samples in relation to CO_2 capture capacity. Compared to the KOH activation biochar samples (61.17% and 62.89% decreased), the capacity of CO_2 adsorption decreased by 31.38%–43.41% for the steam activation biochar samples. From the results of Fig. 6 and Table 2, it seems that

Table 2

The BET surface area, pore volume, and average pore diameter of biochars.

Sample	S_{BET}^a ($m^2 g^{-1}$)	S_{micro}^b ($m^2 g^{-1}$)	S_{meso}^c ($m^2 g^{-1}$)	V_{total} ($cm^3 g^{-1}$)	V_{micro} ($cm^3 g^{-1}$)	Average Pore Diameter (\AA)
BC-Raw	130.5	22.8	137.1	0.17	0.01	52.37
BC-Steam-0.5h	475.1	288.8	297.6	0.42	0.11	36.62
BC-Steam-1.0h	854.7	478.5	604.8	0.89	0.22	42.05
BC-Steam-1.5h	658.2	372.1	488.9	0.69	0.17	41.71
BC-KOH-2:1	411.0	383.8	200.0	0.34	0.18	29.93
BC-KOH-1:1	713.5	585.8	309.0	0.46	0.25	25.76
BC-KOH-1mp	707.4	564.1	308.8	0.46	0.24	26.07

^a BET surface area.^b t-plot method.^c BJH method.**Fig. 5.** (a) CO₂ adsorption ability of differently prepared samples detected by TGA; Correlation between CO₂ capture capacity and (b) BET surface area, (c) micropore surface area, (d) mesopore surface area, (e) micropore volume, (f) total pore volume.

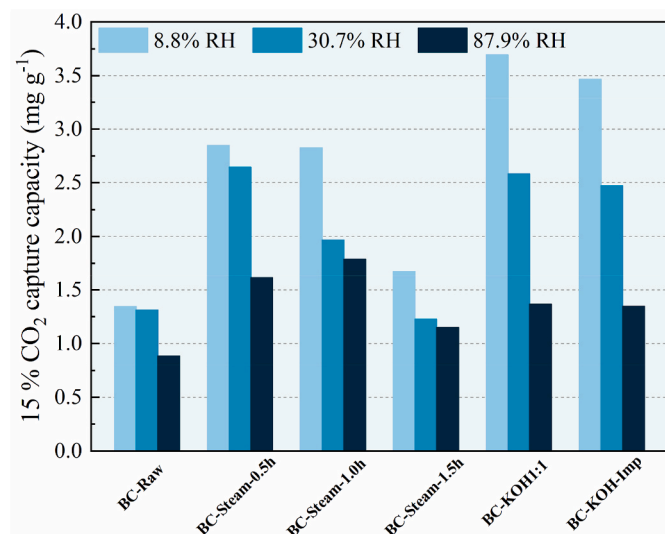


Fig. 6. 15% CO₂ adsorption ability of biochar samples at different RH in the fixed bed detected by the gas analyzer.

moisture significantly affects the porous biochar with a higher ratio of micropores. The steam-activated biochars exhibit more macro- and mesopores, which would demonstrate high rates of CO₂ transportation, whilst the high ratio of micropore shown by KOH-activated biochar provides effective CO₂ adsorption and adequate active sites [49]. Moreover, high N and O content (Table 1) in the KOH-activated biochars could generate more surface functional groups, which can improve the surface polarity of chemical-activated biochar more than that derived from the physical activation. Thereafter, the high polarity of biochar could enhance moisture retention and result in the negative effect of moisture on CO₂ adsorption [38]. Hence, relative humidity has a negative effect on biochar materials that mainly utilize physisorption of CO₂; thus, it is suggested that chemically activated biochars with abundant microporosity and high polarity should require more attention regarding the influence of moisture.

The stability of the prepared biochar was further investigated using BC-Steam-1.0h for 35 cycles of CO₂ adsorption/desorption at 8.8% RH and 87.9% RH. As shown in Fig. 7, the adsorption capacity is maintained at about 2.20 mg g⁻¹ at 8.8% RH. It is indicated that the adsorption and desorption process with temperature swing had little influence on the adsorption capacity at low moisture conditions. This is consistent with the literature demonstrating that biochar had high stability under a dry CO₂ atmosphere [33]. However, when the relative humidity was 87.9%, the stability of BC-Steam-1.0h was reduced from 2.0 mg g⁻¹ to 1.0 mg g⁻¹ after 25 cycles of adsorption/desorption. A pinewood sawdust-derived activated carbon [50] exhibited a stable CO₂ uptake of 1.8 mmol g⁻¹ after nine cycles. In addition, an activated carbon [47] showed CO₂ adsorption capacity decreased by 18% after several cycles. Therefore, competitive water vapor adsorption may not be immediately apparent due to the delayed adsorption of H₂O for biochar with microporous pores as the primary means of adsorption [51]. However, if the adsorption time or the number of cycles is sufficiently long, water vapor molecules will occupy the CO₂ adsorption sites and cause a decrease in adsorption.

Importantly, since the moisture effect of carbon capture has been investigated, reducing the humidity in the flue gas and improving the adaptation of the biochar to work in high moisture conditions is necessary. In practice, removing moisture from the flue gas or air would incur a high cost, and direct air capture may play an important role in reducing atmospheric CO₂. Therefore, biochar modification to increase the surface hydrophobicity need to be improved. Although biochar was mostly hydrophobic, the surface modification would improve the CO₂

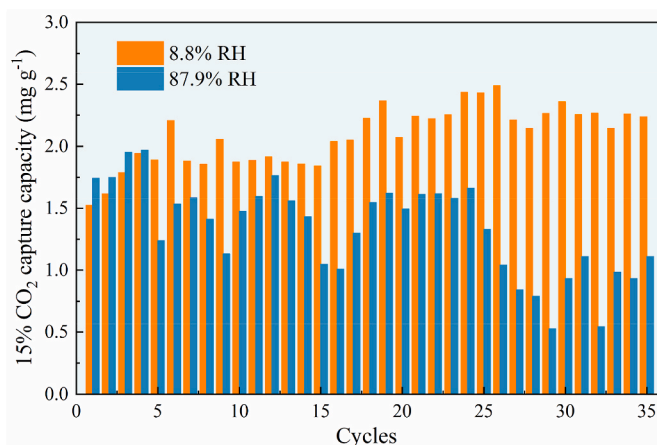


Fig. 7. Stability exploration of BC-Steam-1.0h at 8.8% RH and 87.9% RH in 15% CO₂ atmosphere.

adsorption ability and the hydrophobicity [38]. As reported by Ding et al., the dynamic CO₂ capacity under humid conditions reached a 94% retention rate after modifying the adsorbent with functional groups and organic components (polynaphthylene) [34]. Consequently, introducing polarity functional groups can be an essential method for modifying biochar.

4. Conclusion

Wood pellet derived biochar with different activation methods is demonstrated as a potential sorbent for carbon capture of CO₂. The results illustrate that biochar with a predominantly microporous morphology has a higher CO₂ capture capacity; For example, BC-KOH-1:1 shows the CO₂ uptake of 50.75 mg g⁻¹, and BC-Steam-1.0h exhibits the CO₂ capture capacity of 38.30 mg g⁻¹. Moreover, carbon capture capacity is decreased by 62.89% for all the investigated samples when the relative humidity increased from 8.8% to 87.9%. Indeed, the adequate microporous structure of KOH-activated biochar results in a greater effect of relative humidity on its CO₂ adsorption performance, which suggests that water molecules may occupy the micropores leading to a reduction in CO₂ capture. Furthermore, the stability of CO₂ capture using the BC-Steam-1.0h sample was stable at 8.8% RH, while the capacity of CO₂ capture was largely reduced at 87.9% RH after 35 cycles of adsorption/desorption. Consequently, it is suggested that moisture in the CO₂ source should be pre-removed prior to the carbon capture process, while it is necessary to improve the stability and adsorption efficiency of adsorbents at high relative humidity.

Declaration of competing interest

The authors declare that they have no known competing financial interests or personal relationships that could have appeared to influence the work reported in this paper.

Data availability

The data that has been used is confidential.

Acknowledgment

This project has received funding from the European Union's Horizon 2020 research and innovation programme under the Marie Skłodowska-Curie grant agreement No 823745. UK Catalysis Hub is kindly thanked for the resources and support provided via our membership of the UK Catalysis Hub Consortium and funded by EPSRC grant: EP/R026939/1, EP/R026815/1, EP/R026645/1, EP/R027129/1 or EP/

MO13219/1(biocatalysis). This research has been performed with the use of facilities at the Research Complex at Harwell including scanning electron microscope equipped with Energy Dispersive X-Ray Analyser (SEM-EDX). The authors would like to thank the Research Complex for access and support to these facilities and equipment.

References

- [1] W.D. Nordhaus, To slow or not to slow: the economics of the greenhouse effect, *Econ. J.* 101 (407) (1991) 920–937.
- [2] A.E. Creamer, B. Gao, Carbon-based adsorbents for postcombustion CO₂ capture: a critical review, *Environ. Sci. Technol.* 50 (14) (2016) 7276–7289.
- [3] M.S. Shafeyan, W.M.A.W. Daud, A. Houshmand, A. Arami-Niya, Ammonia modification of activated carbon to enhance carbon dioxide adsorption: effect of pre-oxidation, *Appl. Surf. Sci.* 257 (9) (2011) 3936–3942.
- [4] G.T. Rochelle, Amine scrubbing for CO₂ capture, *Science* 325 (5948) (2009) 1652–1654.
- [5] G. Booras, S. Smelser, An engineering and economic evaluation of CO₂ removal from fossil-fuel-fired power plants, *Energy* 16 (11–12) (1991) 1295–1305.
- [6] T.C. Drage, C.E. Snape, L.A. Stevens, J. Wood, J. Wang, A.I. Cooper, R. Dawson, X. Guo, C. Satterley, R. Irons, Materials challenges for the development of solid sorbents for post-combustion carbon capture, *J. Mater. Chem.* 22 (7) (2012) 2815–2823.
- [7] R. Idem, M. Wilson, P. Tontiwachwuthikul, A. Chakma, A. Veawab, A. Aroonwilas, D. Gelowitz, Pilot plant studies of the CO₂ capture performance of aqueous MEA and mixed MEA/MDEA solvents at the University of Regina CO₂ capture technology development plant and the boundary dam CO₂ capture demonstration plant, *Ind. Eng. Chem. Res.* 45 (8) (2006) 2414–2420.
- [8] H. Demir, G.O. Aksu, H.C. Gulbalkan, S. Keskin, MOF Membranes for CO₂ Capture: Past, Present and Future, *Carbon Capture Science & Technology*, 2022, 100026.
- [9] R.S. Franchi, P.J. Harlick, A. Sayari, Applications of pore-expanded mesoporous silica. 2. Development of a high-capacity, water-tolerant adsorbent for CO₂, *Ind. Eng. Chem. Res.* 44 (21) (2005) 8007–8013.
- [10] J.S. Cha, S.H. Park, S.-C. Jung, C. Ryu, J.-K. Jeon, M.-C. Shin, Y.-K. Park, Production and utilization of biochar: a review, *J. Ind. Eng. Chem.* 40 (2016) 1–15.
- [11] S. Guo, Y. Li, Y. Wang, L. Wang, Y. Sun, L. Liu, Recent Advances in Biochar-Based Adsorbents for CO₂ Capture, *Carbon Capture Science & Technology*, 2022, 100059.
- [12] J. Wang, S. Wang, Preparation, modification and environmental application of biochar: a review, *J. Clean. Prod.* 227 (2019) 1002–1022.
- [13] J. Lehmann, S. Joseph, Biochar for environmental management: an introduction, *Biochar Environ. Manag.: Sci. Technol.* 1 (2009) 1–12.
- [14] B. Santra, L. Ramrakhiani, S. Kar, S. Ghosh, S. Majumdar, Ceramic membrane-based ultrafiltration combined with adsorption by waste derived biochar for textile effluent treatment and management of spent biochar, *J. Environ. Health Sci. Eng.* 18 (2) (2020) 973–992.
- [15] L. Ramrakhiani, A. Halder, A. Majumdar, A.K. Mandal, S. Majumdar, S. Ghosh, Industrial waste derived biosorbent for toxic metal remediation: mechanism studies and spent biosorbent management, *Chem. Eng. J.* 308 (2017) 1048–1064.
- [16] H. Bamdad, K. Hawboldt, Comparative study between physicochemical characterization of biochar and metal organic frameworks (MOFs) as gas adsorbents, *Can. J. Chem. Eng.* 94 (11) (2016) 2114–2120.
- [17] A. Ros, M. Lillo-Ródenas, E. Fuente, M. Montes-Morán, M. Martín, A. Linares-Solano, High surface area materials prepared from sewage sludge-based precursors, *Chemosphere* 65 (1) (2006) 132–140.
- [18] S. Mashhadi, R. Sohrabi, H. Javadian, M. Ghasemi, I. Tyagi, S. Agarwal, V. K. Gupta, Rapid removal of Hg (II) from aqueous solution by rice straw activated carbon prepared by microwave-assisted H₂SO₄ activation: kinetic, isotherm and thermodynamic studies, *J. Mol. Liq.* 215 (2016) 144–153.
- [19] A.M. Dehkoda, E. Gyenge, N. Ellis, A novel method to tailor the porous structure of KOH-activated biochar and its application in capacitive deionization and energy storage, *Biomass Bioenergy* 87 (2016) 107–121.
- [20] R. Azargohar, A. Dalai, Steam and KOH activation of biochar: experimental and modeling studies, *Microporous Mesoporous Mater.* 110 (2–3) (2008) 413–421.
- [21] S.-C. Lee, H.J. Chae, B.Y. Choi, S.Y. Jung, C.Y. Ryu, J.J. Park, J.-I. Baek, C.K. Ryu, J. C. Kim, The effect of relative humidity on CO₂ capture capacity of potassium-based sorbents, *Kor. J. Chem. Eng.* 28 (2) (2011) 480–486.
- [22] Y. Zhang, Z. Lu, M.M. Maroto-Valer, J.M. Andrésen, H.H. Schobert, Comparison of high-unburned-carbon fly ashes from different combustor types and their steam activated products, *Energy Fuel.* 17 (2) (2003) 369–377.
- [23] C. Sun, T. Chen, Q. Huang, M. Zhan, X. Li, J. Yan, Activation of persulfate by CO₂-activated biochar for improved phenolic pollutant degradation: performance and mechanism, *Chem. Eng. J.* 380 (2020), 122519.
- [24] A.K. Sakhiya, A. Anand, P. Kaushal, Production, activation, and applications of biochar in recent times, *Biochar* 2 (3) (2020) 253–285.
- [25] M. Lussier, Z. Zhang, D.J. Miller, Characterizing rate inhibition in steam/hydrogen gasification via analysis of adsorbed hydrogen, *Carbon* 36 (9) (1998) 1361–1369.
- [26] H. Demiral, I. Demiral, B. Karabacakoglu, F. Tümsük, Production of activated carbon from olive bagasse by physical activation, *Chem. Eng. Res. Des.* 89 (2) (2011) 206–213.
- [27] S. Jung, Y.-K. Park, E.E. Kwon, Strategic use of biochar for CO₂ capture and sequestration, *J. CO₂ Util.* 32 (2019) 128–139.
- [28] Y. Ji, C. Zhang, X. Zhang, P. Xie, C. Wu, L. Jiang, A high adsorption capacity bamboo biochar for CO₂ capture for low temperature heat utilization, *Separ. Purif. Technol.* 293 (2022), 121131.
- [29] P.D. Dissanayake, S. You, A.D. Igalavithana, Y. Xia, A. Bhatnagar, S. Gupta, H. W. Kua, S. Kim, J.-H. Kwon, D.C. Tsang, Biochar-based adsorbents for carbon dioxide capture: a critical review, *Renew. Sustain. Energy Rev.* 119 (2020), 109582.
- [30] N. Le-Minh, E.C. Sivret, A. Shammay, R.M. Stuetz, Factors affecting the adsorption of gaseous environmental odors by activated carbon: a critical review, *Crit. Rev. Environ. Sci. Technol.* 48 (4) (2018) 341–375.
- [31] A.D. Igalavithana, S.W. Choi, J. Shang, A. Hanif, P.D. Dissanayake, D.C. Tsang, J.-H. Kwon, K.B. Lee, Y.S. Ok, Carbon Dioxide Capture in Biochar Produced from Pine Sawdust and Paper Mill Sludge: Effect of Porous Structure and Surface Chemistry, *Science of The Total Environment*, 2020, 139845.
- [32] Y. Qiao, S. Zhang, C. Quan, N. Gao, C. Johnston, C. Wu, One-pot synthesis of digestate-derived biochar for carbon dioxide capture, *Fuel* 279 (2020), 118525.
- [33] Y.-C. Chiang, Y.-J. Chen, C.-Y. Wu, Effect of relative humidity on adsorption breakthrough of CO₂ on activated carbon fibers, *Materials* 10 (11) (2017) 1296.
- [34] N. Ding, H. Li, X. Feng, Q. Wang, S. Wang, L. Ma, J. Zhou, B. Wang, Partitioning MOF-5 into confined and hydrophobic compartments for carbon capture under humid conditions, *J. Am. Chem. Soc.* 138 (32) (2016) 10100–10103.
- [35] D. Venturi, D. Grupkovic, L. Sisti, M.G. Baschetti, Effect of humidity and nanocellulose content on Polyvinylamine-nanocellulose hybrid membranes for CO₂ capture, *J. Membr. Sci.* 548 (2018) 263–274.
- [36] Y. Sudaryanto, S.á. Hartono, W. Irawaty, H. Hindarso, S. Ismadji, High surface area activated carbon prepared from cassava peel by chemical activation, *Bioresour. Technol.* 97 (5) (2006) 734–739.
- [37] Y. Liu, Y. Guo, Y. Zhu, D. An, W. Gao, Z. Wang, Y. Ma, Z. Wang, A sustainable route for the preparation of activated carbon and silica from rice husk ash, *J. Hazard Mater.* 186 (2–3) (2011) 1314–1319.
- [38] E.M. Batista, J. Shultz, T.T. Matos, M.R. Fornari, T.M. Ferreira, B. Szpoganicz, R. A. de Freitas, A.S. Mangrich, Effect of surface area and porosity of biochar on water holding capacity aiming indirectly at preservation of the Amazon biome, *Sci. Rep.* 8 (1) (2018) 1–9.
- [39] G.N. Kasozi, A.R. Zimmerman, P. Nkedi-Kizza, B. Gao, Catechol and humic acid sorption onto a range of laboratory-produced black carbons (biochars), *Environ. Sci. Technol.* 44 (16) (2010) 6189–6195.
- [40] B. Adeniran, R. Mokaya, Is N-doping in porous carbons beneficial for CO₂ storage? Experimental demonstration of the relative effects of pore size and N-doping, *Chem. Mater.* 28 (3) (2016) 994–1001.
- [41] M. Plaza, A. González, J. Pis, F. Rubiera, C. Pevida, Production of microporous biochars by single-step oxidation: effect of activation conditions on CO₂ capture, *Appl. Energy* 114 (2014) 551–562.
- [42] M.M. Maroto-Valer, Z. Lu, Y. Zhang, Z. Tang, Sorbents for CO₂ capture from high carbon fly ashes, *Waste Manag.* 28 (11) (2008) 2320–2328.
- [43] C.F. Martín, M.G. Plaza, J. Pis, F. Rubiera, C. Pevida, T. Centeno, On the limits of CO₂ capture capacity of carbons, *Separ. Purif. Technol.* 74 (2) (2010) 225–229.
- [44] C. Zhang, W. Song, G. Sun, L. Xie, J. Wang, K. Li, C. Sun, H. Liu, C.E. Snape, T. Drage, CO₂ capture with activated carbon grafted by nitrogenous functional groups, *Energy Fuel.* 27 (8) (2013) 4818–4823.
- [45] S.-M. Hong, E. Jang, A.D. Dysart, V.G. Pol, K.B. Lee, CO₂ capture in the sustainable wheat-derived activated microporous carbon compartments, *Sci. Rep.* 6 (1) (2016) 1–10.
- [46] M. Idrees, V. Rangari, S. Jeelani, Sustainable packaging waste-derived activated carbon for carbon dioxide capture, *J. CO₂ Util.* 26 (2018) 380–387.
- [47] J.J. Manyà, D. García-Morcate, B. González, Adsorption performance of physically activated biochars for postcombustion CO₂ capture from dry and humid flue gas, *Appl. Sci.* 10 (1) (2020) 376.
- [48] G.O. Wood, J. Stampfer, Adsorption rate coefficients for gases and vapors on activated carbons, *Carbon* 31 (1) (1993) 195–200.
- [49] Y. Zhang, S. Wang, D. Feng, J. Gao, L. Dong, Y. Zhao, S. Sun, Y. Huang, Y. Qin, Functional biochar synergistic solid/liquid-phase CO₂ capture: a review, *Energy Fuel.* 36 (6) (2022) 2945–2970.
- [50] S. Shakharami, A.K. Dalai, J. Soltan, Y. Hu, D. Wang, Selective CO₂ capture by activated carbons: evaluation of the effects of precursors and pyrolysis process, *Energy Fuel.* 29 (11) (2015) 7433–7440.
- [51] M. Plaza, A. González, F. Rubiera, C. Pevida, Evaluation of microporous biochars produced by single-step oxidation for postcombustion CO₂ capture under humid conditions, *Energy Proc.* 63 (2014) 693–702.